First Middle East Conference on Smart Monitoring,
Assessment and Rehabilitation of Civil Structures
8 – 10 February 2011, Dubai, UAE

SMAR 2011

Modeling of RC wall-like columns FRP confinement

G.P. Lignola[1], A. Prota[1], G. Manfredi[1], and E. Cosenza[1]

[1] Department of Structural Engineering, University of Naples "Federico II", Naples, Italy

ABSTRACT: The confinement of Reinforced Concrete (RC) columns represents one of the most promising applications of Fiber Reinforced Polymer (FRP) to civil structures. The majority of studies have been performed on the confinement with FRP of circular columns, where the contribution of composites is fully exploited. A loss of effectiveness occurs in the case of square cross-sections where the presence of the corners reduces the confining action of the FRP jacket. Such problem becomes particularly critical for rectangular columns; despite that, very few studies have been conducted on them. The present paper deals with rectangular columns with high ratio between the sides of the cross-section. Starting from available experimental programs related to wall-like column confinement, it provides a model for the analytical prediction of the effect of confinement on this kind of cross sections. Present outcomes highlighted the influence of the longest/shortest sides ratio on the confined concrete strength ratio.

1 INTRODUCTION

Within the applications of composites in construction, the confinement of RC columns is one of the most common. For both building columns and bridge piers, the strengthening using FRP ensures an easy and fast installation, strength and/or ductility increase, high durability, low impact on the use of the structure, almost no increase of mass and geometrical dimensions of the cross-sections.

The confining action of FRP jackets gives the best performance on circular columns, whose geometrical configuration allows the fibers to be effective on the entire cross-section. A different behavior characterizes square and rectangular columns; in these cases, due to the presence of the corners a part of the cross-section remains unconfined. Similar to the confinement with steel hoops, that loss of effectiveness is modeled with parabolic areas defined by the corners and eventually by longitudinal steel rebars. This still represents an unresolved issue even in terms of code provisions.

Usually confinement does not change the actual failure mode for walls, but it is able to delay bars buckling, restraining also concrete cover spalling, and to let compressive concrete strains attaining larger values, thus resulting in higher load carrying capacity of the member and in significant ductility enhancement.

Experimental campaign conducted on wall-like columns (Prota et al. 2006) confirmed that significant strength increases can be achieved by FRP wrapping: the number of plies does not play a major role on the axial strength while it gives improvements in terms of axial ductility.

The failure of these walls determines the bulging of the FRP laminates occurring at fiber strains far below the ultimate values provided by the manufacturers. A theoretical model to evaluate ultimate FRP strain has been proposed in Lignola et al. (2009a) suggesting an upper bound of the efficiency factor β (because it neglects stress localization and premature failures), assuming the three-dimensional Tsai-Wu failure criterion. To better limit the range of variability of the effective FRP strain in confinement, a second model was proposed (Zinno et al. 2010) to analyze the effect of the stress concentration at the free edge of the FRP jacket. Interlaminar stress can cause premature failure of the FRP wrapping due to separation or delamination, thus limiting the confinement capacity of the FRP wrapping.

1.1 Preliminary Finite Element analysis

A preliminary Finite Element Method (F.E.M.) analysis has been conducted (Lignola et al. 2009b) in the elastic range to evaluate the stress field generated by external wrapping on confined wall members. The arch-shaped paths of the confining stresses rapidly changes in a straight distribution of confinement stress field moving away from the corner.

A slender rectangular cross-section column has been wrapped with an elastic reinforcement with fibers only in the transverse direction and a distributed load has been applied on the top in a displacement control mode. The boundary constraints were only vertical supports and two pairs of supports in the plane of the load to restrain only rigid movement so that the specimen was free to expand laterally.

A cross-section at mid height of the specimen has been extracted and the principal confining stress vector field is plotted in Figure 1. The arch-shaped paths of the confining stresses rapidly changes in a straight distribution moving away from the corners.

Figure 1. FEM elastic vector plot of confining stresses.

2 DERIVATION OF THE NOVEL CONFINEMENT MODEL

The first models proposed at the beginning of last century were based on Coulomb plasticity criterion (e.g. Richart et al. 1928), so they were based on solid mechanics. Richart et al. (1928) proposed a linear relationship between normalized lateral confining pressure f_l/f_{co} and normalized confined concrete strength f_{cc}/f_{co} (Eq. 1) needing the evaluation of the k_1 constant, where f_{co} is the unconfined concrete strength and f_l is the confining pressure.

Further solid mechanic based models (e.g. William & Warnke 1975) have been developed in last decades, for instance based on triaxial plasticity and calibrated experimentally (e.g. Elwi & Murray 1979) and they have been inserted also in international Codes (e.g. ACI 440 as reported in Eq. 2).

Regression analyses of the experimental results lead to models mainly based on the form reported in Eq. 3, where the constants a and b are determined according to best fitting of experimental data (sometimes a and b can be expressed as functions depending also on different parameters).

$$\frac{f_{cc}}{f_{co}} = 1 + k_1 \frac{f_l}{f_{co}} \tag{1}$$

$$\frac{f_{cc}}{f_{co}} = 2.25\sqrt{1 + 7.9\frac{f_l}{f_{co}}} - 2\frac{f_l}{f_{co}} - 1.25 \tag{2}$$

$$\frac{f_{cc}}{f_{co}} = 1 + a\left(\frac{f_l}{f_{co}}\right)^b \tag{3}$$

2.1 Conventional procedures to account for non-circular cross sections

In the case of non circular cross sections, a shape factor, k_e, can be defined as the ratio between the area of "conventional" effectively confined concrete, A_{con}, to the gross sectional area, $A_g=bd$, where b and d are the sides of the cross section. The effective confined area (Figure 2) is conventionally defined using parabolic arc segments extending between the rounded corners of the section. As Figure 2 allows observing, this approach cannot be straightforwardly extended to wall-like slender cross sections because the two parabolas on the long sides would overlap if b<(h-2R)/2 (where R is the rounding radius) and this would result in overestimating the unconfined area since the overlap portion would be counted twice. To avoid this, initial tangents of the parabolas, equal to 45° in original models, were considered parallel to the diagonals of the cross section. In any case an equivalent circular cross section (diameter D) is needed.

In the case of confinement models based on Eq. 1, the shape factor, k_e, can be also adopted to evaluate an "effective" lateral confining pressure. The average strength of confined concrete column (Eq. 4) can be evaluated as the axial capacity N_{cc} (given by the sum of strength contribution of the confined area A_{con} multiplied by f_{cc} and the cover, unconfined, area A_{cov} multiplied by f_{co}) divided by the gross area of the section A_g (equal to $A_{cov}+A_{cov}$):

$$k_e = \frac{A_{con}}{A_g} = 1 - \frac{(b-2r_c)^2 + (d-2r_c)^2}{3bd} \tag{4}$$

$$\overline{f_{cc}} = \frac{N_{cc}}{A_g} = \frac{(f_{co} + k_1 f_l) A_{con} + f_{co} A_{\mathrm{cov}}}{A_g} = \frac{f_{co}(A_{con} + A_{\mathrm{cov}}) + k_1 f_l A_{con}}{A_g} = f_{co} + k_1 f_l \frac{A_{con}}{A_g} \tag{5}$$

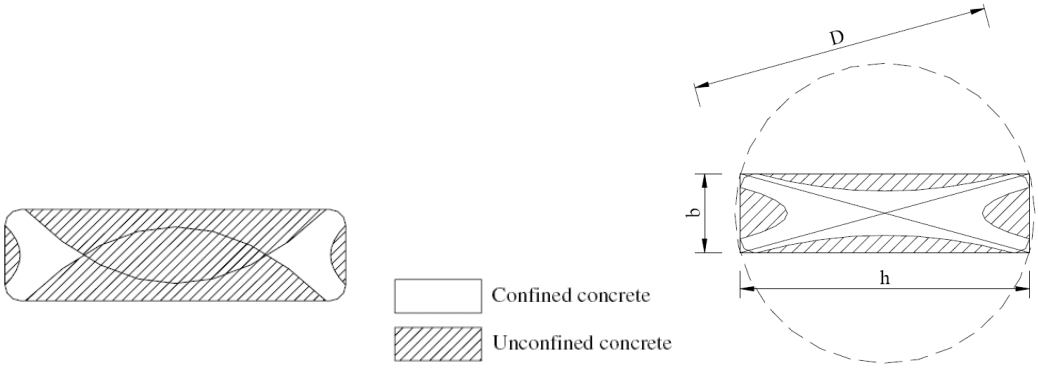

Figure 2. Conventional approaches to compute the effectively confined area.

The "effective", or better, the "equivalent" lateral pressure $k_e f_l$ is the value to be inserted in the confinement model Eq. 1 to obtain directly the average strength of the confined concrete in non circular sections, Eq. 5. It is highlighted that, despite this procedure was extended pragmatically to models based on non linear Eq. 2 and 3, the physical meaning of k_e is not preserved in those cases.

To overcome the limitations of the "conventional" simplified approaches, starting from solid mechanics (ultimate concrete strength surface equations), the following novel model is proposed.

2.2 William and Warnke ultimate concrete strength surface

The plasticity model for concrete under triaxial compression (William & Warnke 1975) is explicitly considered. The ultimate strength surface (Figure 3):

$$\rho = r(\theta,\xi)\cdot f_{co} \tag{6}$$

is formulated in the Haigh–Westergaard stress space defined by the cylindrical coordinates of hydrostatic length (ξ), deviatoric length (ρ) and Lode angle (θ).These coordinates are functions of the invariants (I_1, J_2, J_3) of the principal stress tensor components: $\sigma_1 < \sigma_2 < \sigma_3(=f_{cc})$, according to the following equations:

$$\xi = \frac{I_1}{3} \qquad I_1 = \sigma_1 + \sigma_2 + \sigma_3 \tag{7}$$

$$\rho = \sqrt{\frac{2J_2}{5}} \qquad J_2 = \frac{1}{6}\left[(\sigma_1-\sigma_2)^2 + (\sigma_2-\sigma_3)^2 + (\sigma_3-\sigma_1)^2\right] \tag{8}$$

$$\cos\theta = \frac{3\sqrt{3}}{2}\frac{J_3}{J_2^{3/2}} \qquad J_3 = \left(\sigma_1 - \frac{I_1}{3}\right)\left(\sigma_2 - \frac{I_1}{3}\right)\left(\sigma_3 - \frac{I_1}{3}\right) \tag{9}$$

The Rendulic and deviatoric views of the surface are shown in Figure 3. The surface has curved meridians and the generators are approximated by second-order parabolas along θ=0° (tensile meridian) and θ=60° (compressive meridian) with a common apex at the hydrostatic axis. Where:

$$r(\theta,\xi) = \frac{2r_c\left(r_c^2 - r_t^2\right)\cos\theta + r_c\left(2r_t - r_c\right)\sqrt{4\left(r_c^2 - r_t^2\right)\cos^2\theta + 5r_t^2 - 4r_c r_t}}{4\left(r_c^2 - r_t^2\right)\cos^2\theta + \left(2r_t - r_c\right)^2} \tag{10}$$

$$\cos\theta = \frac{2\sigma_1 - \sigma_2 - \sigma_3}{\sqrt{12J_2}} \tag{11}$$

The parabolic meridians r_c and r_t are the control parameters; they were calibrated by Elwi & Murray (1979) on five control points based on Schikert & Winkler (1977) experimental data and they are expressed as:

$$r_c = 0.095248 + 0.891175\left(\frac{\xi}{f'_{co}}\right) - 0.244420\left(\frac{\xi}{f'_{co}}\right)^2 \tag{12}$$

$$r_t = 0.053627 + 0.512079\left(\frac{\xi}{f'_{co}}\right) - 0.038226\left(\frac{\xi}{f'_{co}}\right)^2 \quad (13)$$

In the ultimate surface equation the only unknown is σ_3 (=f_{cc}) and it can be iteratively evaluated.

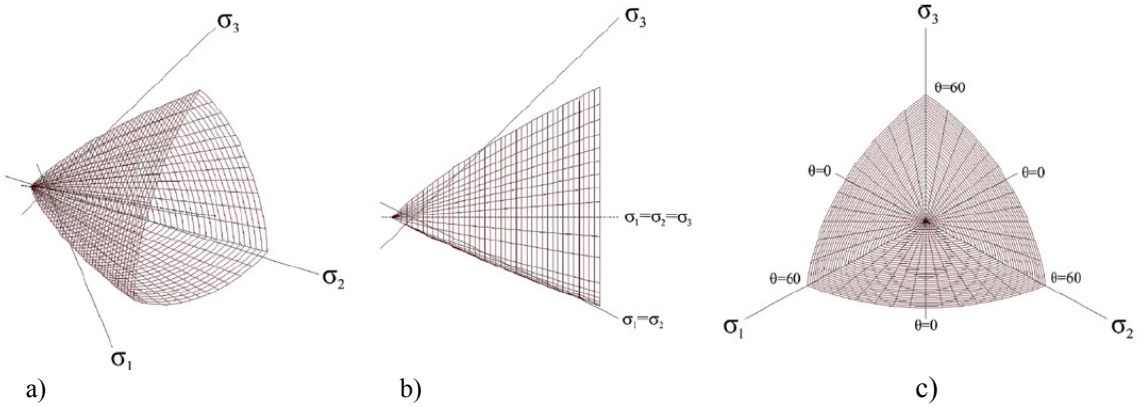

a) b) c)

Figure 3. Ultimate strength surface (a); in the Rendulic plane (b); in the deviatoric plane (c)

2.3 Proposed Confinement Model

Even though a refined nonlinear confinement model was provided for the analysis of circular and noncircular RC columns (e.g., Lignola et al. 2010), to provide a direct, practical tool, oriented to the profession, a simplified confinement model was also provided for wall-like cross-sections (the arch-shaped path of confining stresses was seen to rapidly change in a straight field moving away from the corners). According to this alternative simplified approach, which gives rather accurate results despite the heavily reduced computational effort (no solution is needed of complex equations), the confining stress field is only parallel to the longer side of the cross-section, thus neglecting the confinement in the shorter direction ($\sigma_1 = 0$), the average confining pressure ($\sigma_2 = f_l$) can be assumed equal to:

$$f_l = 2\frac{t_{frp} E_f \varepsilon_{FRP}}{b} \quad (14)$$

assuming cross-section height h > base b. In Eq. 14, t_{frp} is the total thickness of FRP wrapping, E_f and ε_{FRP} are Young modulus and design strain of FRP, respectively. Previous equation is based on the equilibrium according to the free body diagram in Figure 4, where f_{frp} is the stress in the FRP equal to $E_f \varepsilon_{FRP}$.

Assuming zero stress for the minimum principal stress, confining pressure f_l equal to the intermediate principal stress, f_{cc} as the maximum principal stress, the following approximated equation is derived by the concrete ultimate strength surface solution:

$$\frac{f_{cc}}{f_{co}} = 1 + 1.42\frac{f_l}{f_{co}} - 1.40\left(\frac{f_l}{f_{co}}\right)^2 + 0.30\left(\frac{f_l}{f_{co}}\right)^3 \quad (15)$$

where f_l/f_{co}<1.3, otherwise it would result f_l>f_{cc}.

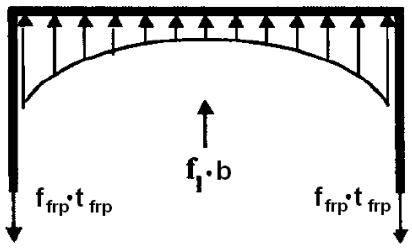

Figure 4. Free body diagram to evaluate the average confining pressure in concrete.

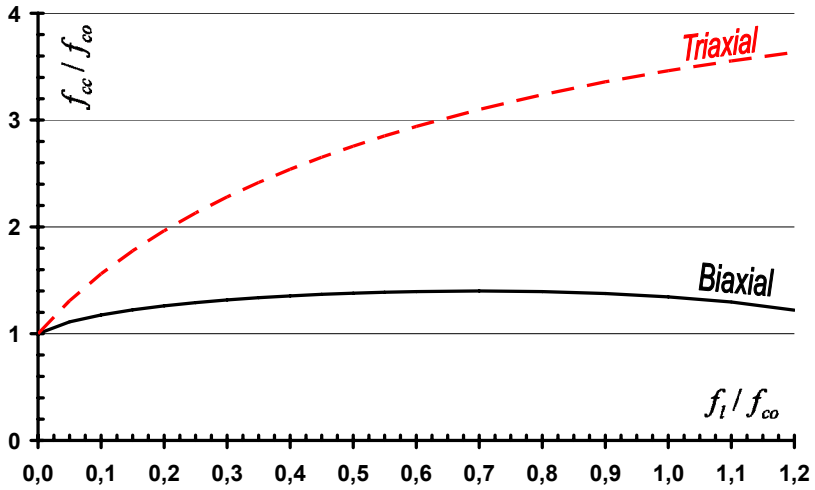

Figure 5. "Biaxial" and "Triaxial" confinement.

In figure 5 is the comparison between the "Triaxial" confinement for concrete (e.g. uniform confining pressure in cylindrical concrete confined members) and the "Biaxial" confinement considered in present case. It is highlighted that the well-known Eq. 2 is the closed form solution for ultimate strength surface (Eq. 6) when $\sigma_1 = \sigma_2 = f_l$.

It is highlighted that in any case, for "Biaxial" confinement, the increase in concrete strength, f_{cc}/f_{co}, is always smaller than 1.5.

3 EXPERIMENTAL VALIDATION OF PROPOSED MODEL

To validate the proposed model, the results available in a database of experimental tests on wall-like columns are compared with analytical predictions of the proposed model.

Experimental tests reported in Tan (2002), Maalej et al. (2003), Prota et al. (2006) and Nardone (2009) provided not only the strength increment, but also the ultimate strain recorded at failure in the FRP.

3.1 FRP strain according to manufacturer ultimate strain

In Figure 6 is the comparison of theoretical predictions and experimental results assuming for the FRP the flat coupon test strength (i.e. ultimate values provided by the manufacturers). This means that failure for FRP fibers is expected at ultimate for this kind of columns. Even if it is a consolidated approach, most of the experimental tests evidenced that the failure of these walls

determines the bulging of the FRP laminates occurring at fiber strains far below the ultimate values provided by the manufacturers (Prota et al. 2006). The proposed results are far below the "triaxial" theoretical confinement curve (as expected), but they are also very different from the proposed "biaxial" theoretical confinement curve, mainly in terms of horizontal distance (i.e. f_l/f_{co} wrong point), rather than in terms of vertical distance (i.e. strength increment, f_{cc}/f_{co}, is almost compatible and usually smaller than 1.5). In this case the average overestimation of the proposed model is about 39 % with a coefficient of variation equal to 49 %. In any case the experimental points are totally inconsistent.

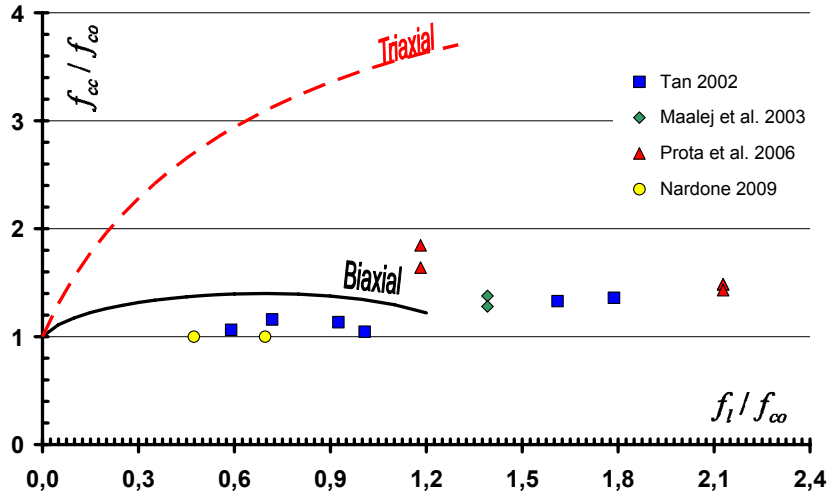

Figure 6. Theoretical vs. Experimental comparison (FRP strain according to manufacturer data).

3.2 Effective FRP ultimate strain

According to previous consideration on f_l possible mistakes, looking carefully at experimental results in terms of FRP strain at failure, the proposed model was applied again considering now, in Eq. 14, the effective ultimate strain recorded during experimental tests. The comparison is shown in Figure 7.

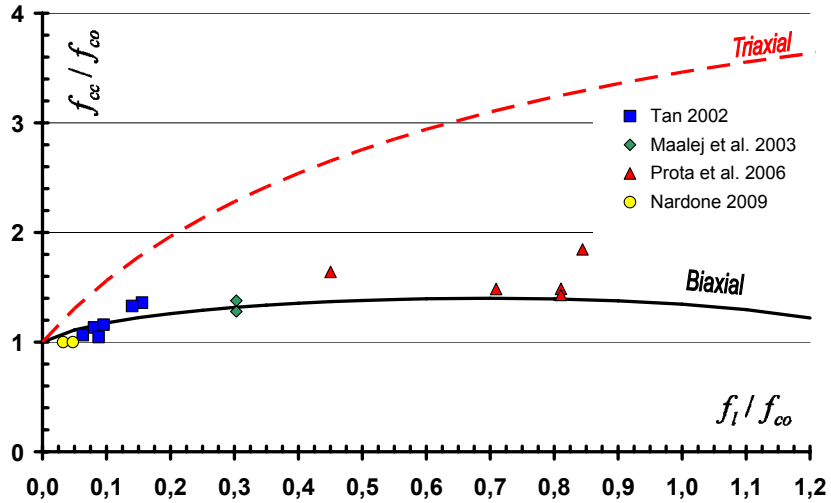

Figure 7. Theoretical vs. Experimental comparison (effective FRP ultimate strain).

In this case the average overestimation of the proposed model is about 5.7 % with a coefficient of variation equal to 10 %.

4 CONCLUSIONS

Assuming a circular cross section, the confinement is uniform and "triaxial", while moving to square and rectangular cross sections, the confining pressure varies inside the cross section, becoming almost parallel to the longest side of the section. Significant differences can be found in the stress state of concrete becoming almost "biaxial". The proposed model for wall-like columns represents, at the same time, a lower bound for the confinement of non circular cross sections.

A model for the analytical prediction of the effect of confinement on slender wall-like cross sections is proposed and good agreement are found between experimental and numerical outcomes only if proper values of FRP strain at ultimate are provided.

In this sense, the issue of the "effective" FRP strain is still open and further research is needed in this field.

4.1 References

ACI Committee 440. 2002. *Guide for the Design and Construction of Externally Bonded FRP Systems for Strengthening Concrete Structures*, ACI440.2R-02 American Concrete Institute

Elwi, AA, and Murray, DW. 1979. A 3-D hypoelastic concrete constitutive relationship. *Journal of Engineering Mechanics Division, ASCE*, 105(4): 623–641.

Lignola, GP, Prota, A, Manfredi, G, and Cosenza, E. 2009a. Evaluation Of Effective Ultimate Strain Of FRP Confinement Jackets Applied On Circular RC Columns. *Proc. 9th International Symposium on Fiber Reinforced Polymer Reinforcement for Concrete Structures FRPRCS9*. Sydney, Australia.

Lignola, GP, Prota, A, Manfredi, G, and Cosenza, E. 2009b. Non linear modeling of RC hollow piers confined with CFRP. *ELSEVIER Composites Structures*, 88(1): 56-64.

Lignola, GP, Prota, A, Manfredi, G, and Cosenza, E. 2010. Non linear refined modeling of FRP Confinement on Prismatic RC Columns. *14th European Conference on Earthquake Engineering*. Ohrid, Republic of Macedonia.

Maalej, M, Tanwongsval, S, and Paramasivam, P. 2003. Modelling of rectangular RC columns strengthened with FRP. *Cement & Concrete Composites*, 25: 263-276.

Nardone, F. 2009. *Colonne in scala reale in c.a. confinate con FRP: Indagine sperimentale e modellazione analitica.*. Ph.D. Thesis in Seismic Risks (XXII cycle): Università degli Studi di Napoli "Federico II", Napoli, Italy. *In Italian*

Prota, A, Manfredi, G, and Cosenza, E. 2006. Ultimate behaviour of axially loaded RC wall-like columns confined with GFRP. *ELSEVIER Composites: Part B*, 37: 670-678.

Richart, FE, Brandtzaeg, A, and Brown, RL. 1928. *A Study of the Failure of Concrete Under Combined Compressive Stresses*. Univ. of Illinois Engineering Experimental Station, Champaign, Ill, Bulletin 185

Schickert, G, and Winkler, H. 1977. *Results of test concerning strength and strain of concrete subjected to multiaxial compressive stress*, Deutsche Ausschuss för Stahlbeton, 277, 123 pages.

Tan, KH. 2002. Strength enhancement of rectangular RC columns using FRP. *Journal of Composites for Construction, ASCE*, 6(3): 175-183.

Teng, JG, Huang, YL, Lam, L and Ye, LP. 2007. Theoretical model for fiber reinforced polymer-confined concrete. *ASCE Journal of Composites for Construction*, 11(2): 201-210.

William, KJ, and Warnke, EP. 1975. Constitutive Model for the Triaxial Behavior of Concrete. *International Association for Bridge and Structural Engineering Proceedings*, 19:1-30.

Zinno, A, Lignola, GP, Prota, A, Manfredi, G, and Cosenza, E. 2010. Influence of free edge stress concentration on effectiveness of FRP confinement. *ELSEVIER Composites: Part B*, 41(7): 523-532.